Vacuum 178 (2020) 109384

Contents lists available at ScienceDirect

Vacuum

journal homepage: http://www.elsevier.com/locate/vacuum

Thermoelectric materials and devices fabricated by additive manufacturing

Yong Du [a,*], Jiageng Chen [a], Qiufeng Meng [a], Yunchen Dou [a], Jiayue Xu [a,**], Shirley Z. Shen [b]

[a] School of Materials Science and Engineering, Shanghai Institute of Technology, 100 Haiquan Road, Shanghai, 201418, China
[b] CSIRO Manufacturing, Private Bag 10, Clayton South, VIC, 3169, Australia

ARTICLE INFO

Keywords:
Additive manufacturing
Thermoelectric materials
Thermoelectric properties

ABSTRACT

Thermoelectric (TE) materials can directly convert thermal energy into electrical energy and vice versa. However, the conversion efficiencies of TE power generators and coolers are lower than those of traditional electric generators and refrigerators. Precision control of TE material composition, development of new preparation technologies, and optimization of the geometric structures of devices are the primary strategies for enhancing conversion efficiencies. Additive manufacturing (3D printing) is a bottom-up synthesis approach that can produce complex geometries from three-dimensional model data. This technique has many advantages, such as rapid fabrication of complex geometric structures, mass-customization saving raw materials and time, and reduced fixturing and tooling. Therefore, additive manufacturing is particularly suitable for fabrication of almost any shape of TE material or device. Additive manufacturing is a rapidly expanding topic in research and technology. The application of additive manufacturing techniques to TE materials and devices is in its infancy but is an emerging topic. This article provides a brief review of the research progress and existing problems in TE materials and devices fabricated by additive manufacturing. Several additive manufacturing techniques for TE materials and devices are highlighted: stereolithography apparatus, fused deposition modelling, selective laser melting/sintering, and solution printing. The challenges of additive manufacturing techniques for TE materials are also discussed.

1. Introduction

Thermoelectric (TE) materials can directly convert heat to electrical power and vice versa, based on the Seebeck effect discovered by German scientist Thomas Johann Seebeck in 1821 and the Peltier effect discovered by French scientist Jean Charles Athanase Peltier in 1834 [1,2]. Devices made of TE materials have many advantages such as small size, no sound, no gas pollution, and high stability [3–7]. TE materials mainly include inorganic TE materials [8–12], conducting polymer TE materials [13–15], and inorganic-polymer TE composites [16–21]. The primary factor limiting widespread application of TE power generators and coolers is their low conversion efficiency [22]. In a TE power generator, the TE property of the material (estimated by the dimensionless figure of merit, $ZT = S^2\sigma T/\kappa$, where S is the Seebeck coefficient, σ is the electrical conductivity, κ is the thermal conductivity, and T is the absolute temperature [23]), the temperature difference between the hot and cold sides, and the geometric structure of the power generator significantly affect its conversion efficiency.

Normally, the shape of heat sources is non-planar, which limits the application of TE power generators made of traditional TE bulk materials (Bi-Te-, Sn-Se-, or Pb-Te-based alloys) prepared via commonly used processes, such as hot pressing [24–26], spark plasma sintering [27,28], and zone melting [29,30], because the as-prepared TE bulk materials and devices are rigid (Fig. 1a). Thus, new processes for preparation of non-planar TE devices are urgently needed (Fig. 1b).

Additive manufacturing (3D printing) is a bottom-up synthesis approach that can produce complex structures from three-dimensional model data. It has many obvious advantages such as rapid fabrication of complex geometric structures, mass-customization, raw material conservation, reduced fixturing and tooling, and shorter cycle time for design and manufacturing [31–38]. Thus, additive manufacturing is particularly suitable for fabrication of any irregular shaped TE material and device and has advantages over traditional TE material preparation technologies such as spark plasma sintering and hot-pressing methods. Additive manufacturing for TE materials and devices has generated less interest than in other fields, but is emerging rapidly [38–43]. However,

* Corresponding author.
** Corresponding author.
E-mail addresses: ydu@sit.edu.cn (Y. Du), xujiayue@sit.edu.cn (J. Xu).

https://doi.org/10.1016/j.vacuum.2020.109384
Received 1 March 2020; Received in revised form 4 April 2020; Accepted 7 April 2020
Available online 6 May 2020

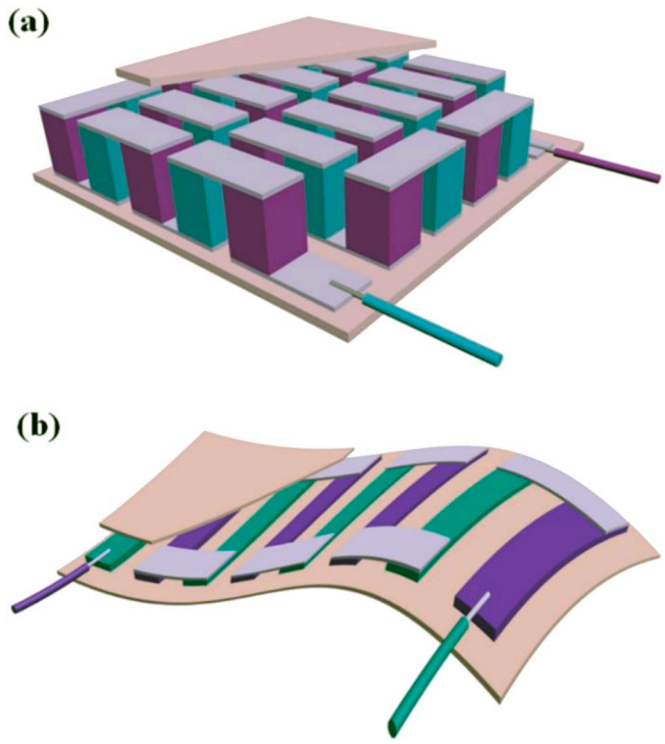

Fig. 1. Schematic of (a) traditional TE power generation and (b) flexible TE power generation.

no systemic summary of TE materials and devices prepared by additive manufacturing has been reported. This article provides a brief overview of TE materials and devices prepared by additive manufacturing. The advantages and disadvantages of different additive manufacturing technologies are summarized, the research progress of TE materials and devices prepared by additive manufacturing is reviewed, and the challenges, perspectives, and outlook of additive manufacturing are discussed.

2. Additive manufacturing

The differences between additive manufacturing and traditional subtractive manufacturing or formative manufacturing are illustrated in Fig. 2. 'Additive manufacturing' is a general term encompassing many techniques, including stereolithography apparatus (SLA), fused deposition modeling (FDM), selective laser melting (SLM)/selective laser sintering (SLS), and solution printing (SP) [44–48]. Each additive manufacturing technique has its own applied range, limitations, and benefits in producing prototype models [49]. Table 1 summarizes the principles, consumable materials, advantages, and disadvantages of typical additive manufacturing techniques.

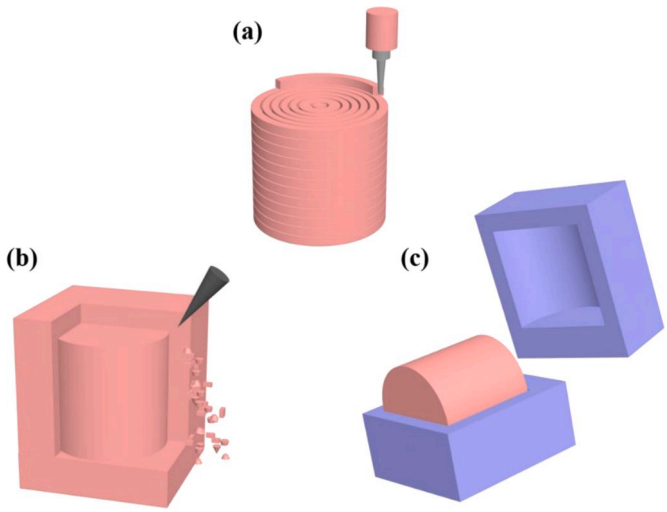

Fig. 2. Comparison of (a) additive, (b) subtractive, and (c) formative manufacturing techniques.

3. Additive manufacturing for TE materials and devices

3.1. Stereolithography apparatus (SLA)

Generally, the SLA process photocures photoresins layer by layer using laser scanning to form the designed geometric structure. The SLA process is shown in Fig. 3 [54].

He et al. [39] dispersed $Bi_{0.5}Sb_{1.5}Te_3$ in the photoresins and fabricated the bulk materials using a mimicked SLA process before annealing at 350 °C in argon gas for 6 h (Fig. 4). The electrical conductivity, Seebeck coefficient, and thermal conductivity of the prepared bulk material with 60 wt% $Bi_{0.5}Sb_{1.5}Te_3$ were ~47 - 33 S/cm, ~148 - 181 μV/K, and ~0.27–0.81 $Wm^{-1}K^{-1}$, respectively, in the measured temperature range (~43 - 300 °C). As a result, a *ZT* value of 0.12 was obtained at 43 °C.

The disadvantages of preparation of TE materials using the SLA process are: (1) the types of photoresins are limited, which restricts application of the SLA process; (2) the content of inorganic TE materials in the photoresins must be strictly controlled. Content that is too low leads to composites with very low electrical conductivity or transfer to insulators. Content that is too high leads to forming issues.

Table 1
Principles, consumable materials, advantages and disadvantages of typical additive manufacturing techniques.

Technique	Principle	Consumable materials	Advantages	Disadvantages
SLA [39, 50]	To photocure the photoresins layer by layer under laser scanning according to a set path	Photoresins	Intricate internal structures can be printed	Photoresin types are limited
FDM [40, 41,44, 50,51]	To melt a solid thermoplastic filament and deposit successive layers to form the designed shape	Acrylonitrile butadiene styrene, polylactic acid, etc., solid thermoplastic filaments	Support/ platform not required	Filaments need to be prepared, high temperature process, nozzle clogging
SLM/SLS [38,52, 53]	To use selective high-energy lasers to sinter powders together to form the designed shape	Polymer powders, metal powders	Support not required	Surface quality and speed require a balance, high cost
SP [42,43, 50]	To use inks to print the designed shape layer by layer	Strands of paste/viscous material in solution form	Suitable for solutions containing polymers, inorganic-polymer composites, and inorganic inks	Shrinkage may occur in final products

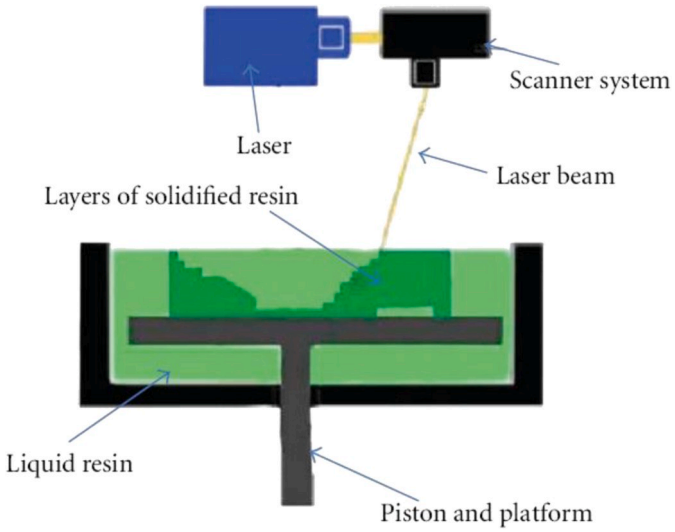

Fig. 3. Stereolithography. From Ref. [54]. Used under CC-BY license.

3.2. Fused deposition modeling (FDM)

FDM involves melting a solid thermoplastic filament and depositing successive layers to form the designed shape (Fig. 5 [51]). The first step for fabrication of TE materials and devices using FDM is to prepare the filaments. The most commonly used thermoplastic filaments are made of acrylonitrile butadiene styrene (ABS), polylactic acid (PLA), polyurethane (PU), polycarbonate (PC), polyvinyl alcohol (PVA), and their corresponding inorganic-polymer composites [55–57]. Wang et al. [58] prepared $Bi_{0.5}Sb_{1.5}Te_3$/multi-walled carbon nanotubes/PLA (BST/MWCNTs/PLA) composite wires by extruding at 170 - 185 °C according to the loading of BST (Fig. 6). Electrical conductivity, Seebeck coefficient, thermal conductivity, and *ZT* value of ~3.5 S/cm, ~178.7 μV/K, 0.31 $Wm^{-1}K^{-1}$, and 0.011 were achieved, respectively, for composite wires with 81.3 wt% BST and 4 wt% MWCNTs at room temperature. The *ZT* value (0.011) is much higher than that of BST/PLA composite wires with 87.5 wt% BST (0.006 at room temperature) prepared using the same procedure.

Once the filaments are prepared, the TE materials and devices can be produced using an FDM process. Aw et al. [41] prepared conductive acrylonitrile butadiene styrene (CABS, a mixture of acrylonitrile butadiene styrene and carbon black residue)/ZnO composites using an FDM process with 14 wt% ZnO. The effects of printing parameters such as infill density and printing pattern on the TE properties of the composites were also investigated. Electrical conductivity, Seebeck coefficient, thermal conductivity, and *ZT* value of $\sim 3.74 \times 10^{-6}$ S/cm, 2.2 μV/K, 0.317 $Wm^{-1}K^{-1}$, and 5.7×10^{-5} for composites with 100% infill density and line printing pattern were obtained, respectively, at room temperature. The relatively low *ZT* value of the material is mainly due to the low electrical conductivity and Seebeck coefficient of the as-prepared composites.

Oztan et al. [40] prepared Bi_2Te_3/ABS filaments with 80 wt% Bi_2Te_3 by extruding at 220 °C after mixing Bi_2Te_3 powders and ABS powders. Bi_2Te_3/ABS composites were fabricated by an FDM method before heat treatment and sintering at different temperatures from 450 °C to 575 °C. A maximum *ZT* value of 0.54 was obtained at room temperature for composites sintered at 500 °C (Fig. 7).

FDM is the most popular method for fabrication of TE materials. However, two facets of the process should be improved to enhance the *ZT* value: (1) the thermoplastic filaments normally need to be extruded at approximately 200 °C, and the temperature for printing TE materials using FDM is even higher than 200 °C. During the process, the inorganic TE materials, Bi-Te- and Pb-Te-based alloys, are easily oxidized. Atmospheric protection may be an effective means of reducing or eliminating the oxidation of inorganic TE materials; (2) the heat treatment and sintering process require optimization because the heat treatment temperature, time, and atmosphere significantly affect the TE properties of the inorganic materials, and in turn influence the TE properties of the printed materials.

3.3. Selective laser melting (SLM)/selective laser sintering (SLS)

SLM/SLS processes usually use selective high-energy lasers to sinter powders together to form the designed product. One of the differences between SLM and SLS is that the SLM process is always used for metal powders, while the SLS process can be used for polymers, metals, and alloy powders [46]. Fig. 8 illustrates the SLM process [59].

Mao et al. [53] prepared n-type $Bi_2Te_{2.7}Se_{0.3}$ with an SLM process using the as-prepared $Bi_2Te_{2.7}Se_{0.3}$ powders, fabricated by self-propagating high-temperature synthesis before grinding with a

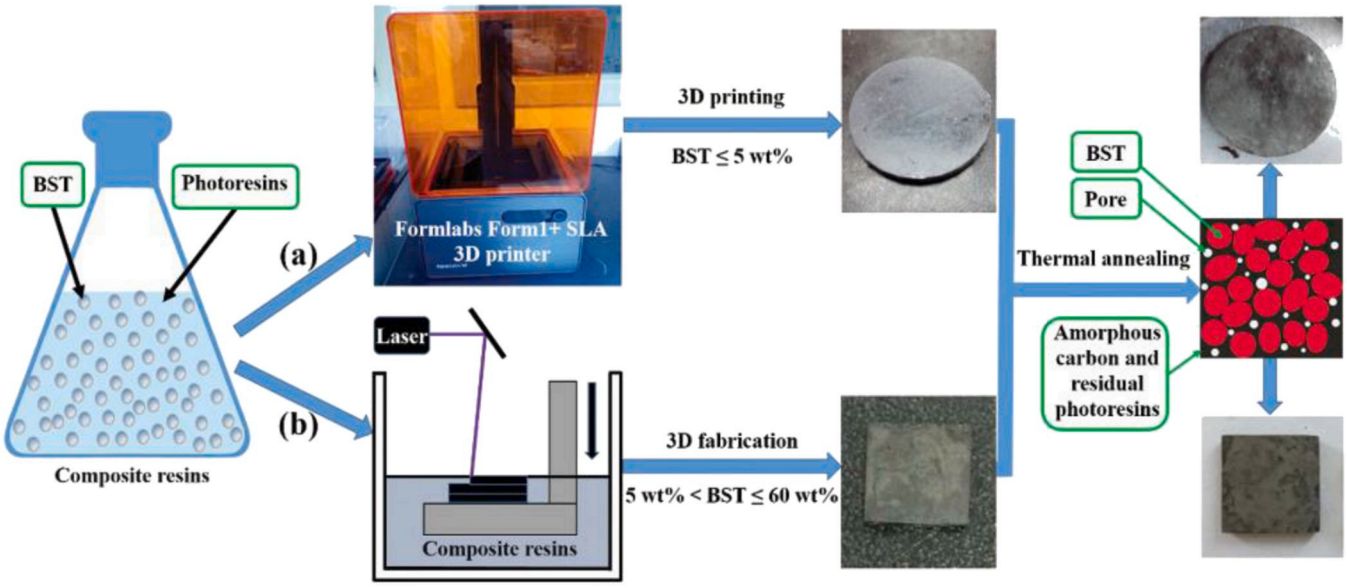

Fig. 4. Schematic routes of (a) 3D printing and (b) 3D fabrication of $Bi_{0.5}Sb_{1.5}Te_3$ samples mixed with Formlabs Clear Photoresins and customized phtoresins, respectively, followed by thermal annealing. From Ref. [39]. © John Wiley and Sons, used with permission.

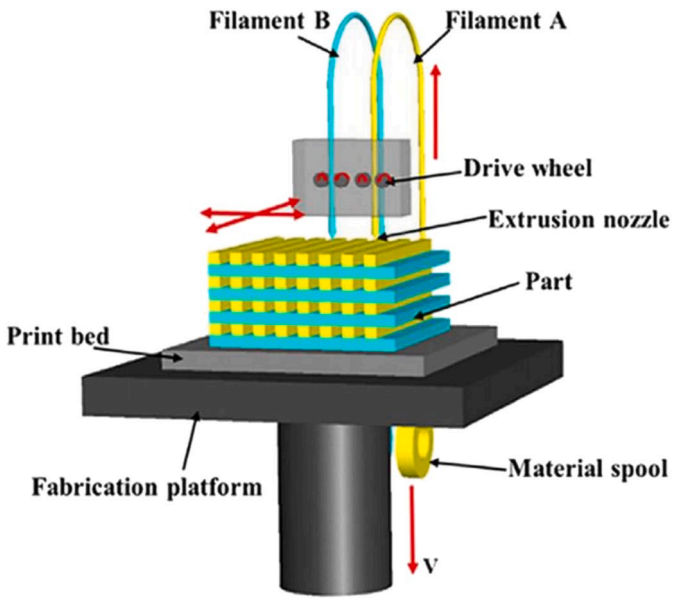

Fig. 5. Schematic representation of a typical FDM setup. From Ref. [51]. © Elsevier, used with permission.

planetary ball mill. The laser energy density of the SLM process significantly affects the forming quality, microstructure, phase composition, and TE properties of the as-prepared materials. A *ZT* value of 0.84 at 400 K was obtained for the n-type $Bi_2Te_{2.7}Se_{0.3}$ by optimizing the laser energy density. Qiu et al. [60] prepared p-type $Bi_{0.4}Sb_{1.6}Te_3$ bulk material via an SLM process, and a *ZT* value of 1.1 at 316 K was obtained. Shi et al. [38] reported a porous $Bi_{0.5}Sb_{1.5}Te_3$ material with an SLS process using 100 mesh $Bi_{0.5}Sb_{1.5}Te_3$ powders, achieving a *ZT* value of ~1.29 at 54 °C. The as-prepared porous $Bi_{0.5}Sb_{1.5}Te_3$ materials exhibited a higher *ZT* value than a commercial bulk material, mainly due to lower thermal conductivity (0.27 $Wm^{-1}K^{-1}$ at 54 °C) than the commercial bulk material (>1.5 $Wm^{-1}K^{-1}$ at 54 °C) (Fig. 9). The decreased thermal conductivity of the as-prepared porous $Bi_{0.5}Sb_{1.5}Te_3$ materials resulted from boundaries and defects formed in the SLS process and porous structures in the materials.

TE materials prepared by SLM/SLS processes exhibit higher *ZT* values than materials prepared by SLA and FDM methods. This is mainly because the insulating polymers are not necessarily needed as binders during the SLM/SLS processes. However, SLM/SLS processes generally require heating to a temperature that fully or nearly melts the powders (e.g. > 500 °C for Bi-Te- based alloys), which may introduce some impure phases or oxidation.

3.4. Solution printing (SP)

SP is one of the most convenient additive manufacturing methods. SP uses inks to print samples layer by layer. During or after the printing process, printed samples are dried on a non-heated or heated substrate. Kim et al. [42] prepared all-inorganic viscoelastic inks using Sb_2Te_3 chalcogenidometallate ions as inorganic binders for p-type $Bi_{0.4}Sb_{1.6}Te_3$ and n-type $Bi_2Sb_{2.7}Se_{0.3}$ particles, and fabricated the corresponding materials using an SP process. *ZT* values of 0.9 for $Bi_{0.4}Sb_{1.6}Te_3$ materials at 125 °C and 0.6 for $Bi_2Sb_{2.7}Se_{0.3}$ materials at 170 °C were

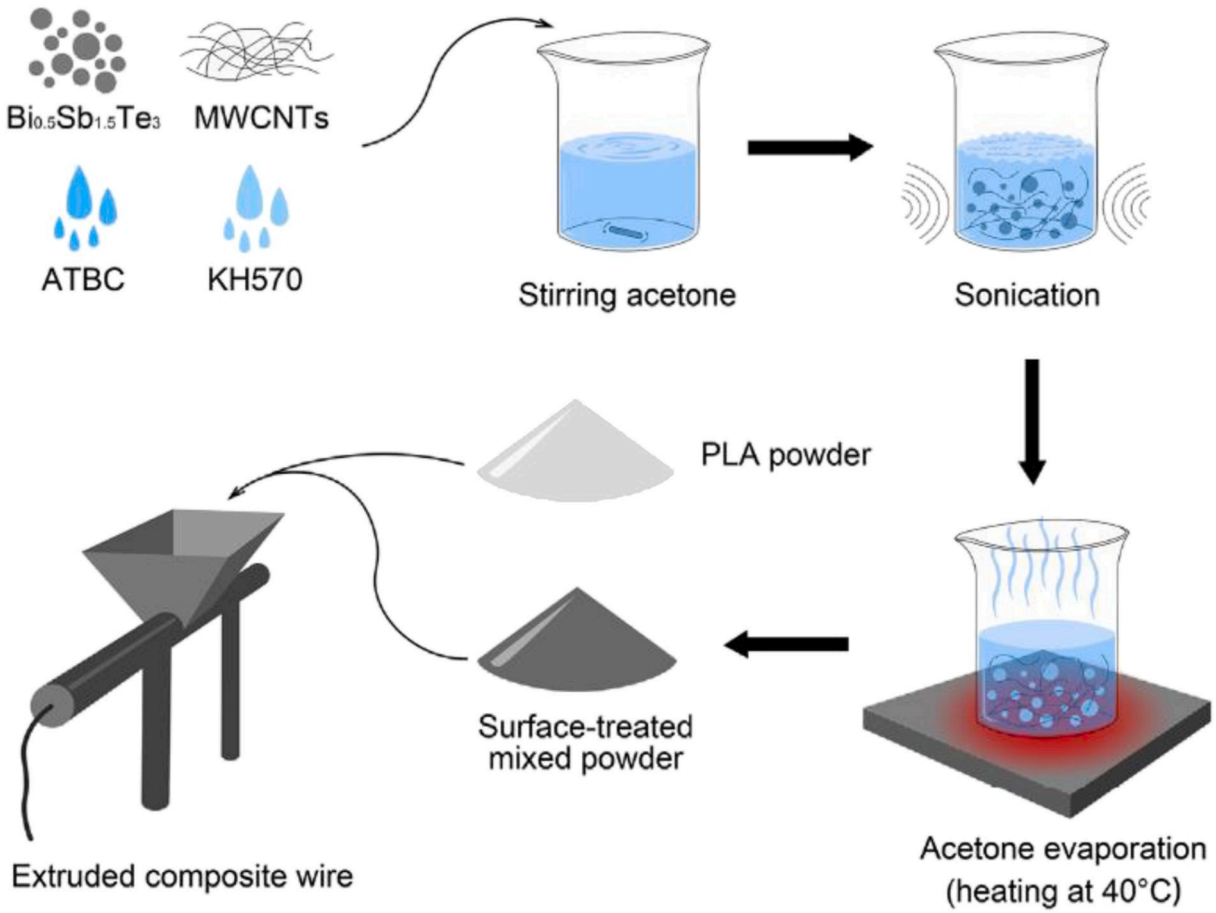

Fig. 6. Synthetic processes of BST/PLA composite wires (KH570 and ATBC represent 3-(trimethoxysilyl)propyl methacrylate and tributyl 2-acetylcitrate, respectively). From Ref. [58]. © Elsevier, used with permission.

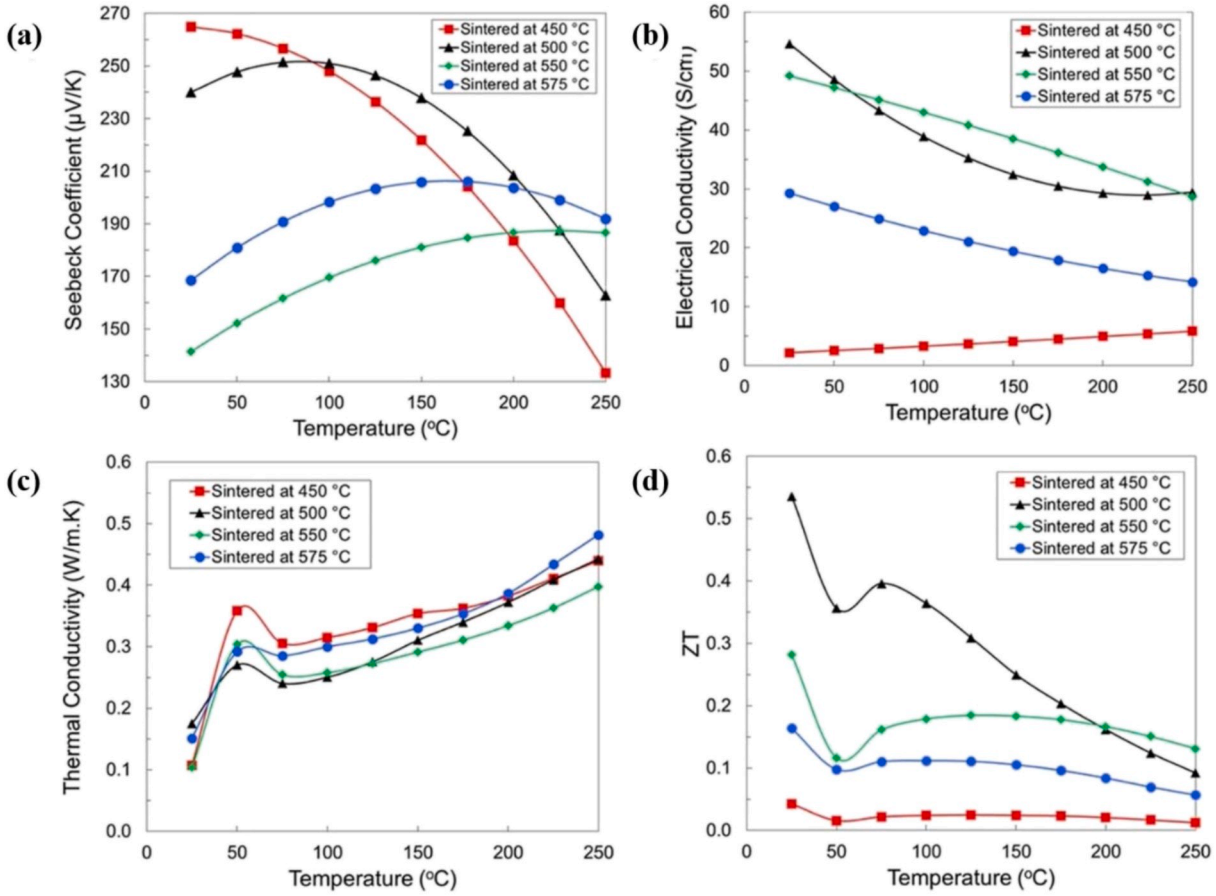

Fig. 7. Temperature dependence of thermoelectric properties of specimens sintered at four different temperatures: (a) Seebeck coefficient, (b) electrical conductivity, (c) thermal conductivity, and (d) dimensionless figure of merit. From Ref. [40]. © Elsevier, used with permission.

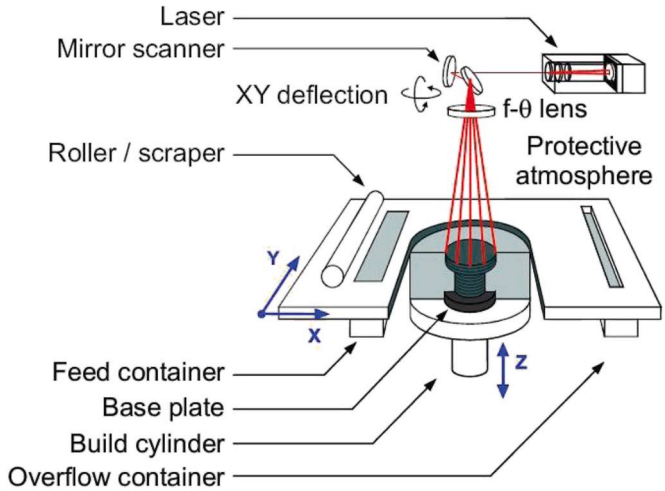

Fig. 8. A schematic view of the SLM process. From Ref. [59]. © Elsevier, used with permission.

achieved. An output power density of 1.42 $mWcm^{-2}$ at a temperature difference of 39 °C was achieved for a TE power generator fabricated using three pairs of the as-prepared n-type and p-type TE half-ring materials. Su et al. [61] fabricated p-type $Bi_{0.5}Sb_{1.5}Te_3$/polyvinylpyrrolidone (PVP) and n-type Bi_2Te_3/PVP composites by a direct-writing 3D printing method. *ZT* values of 0.104 (p-type) and 0.11 (n-type) were obtained at 25 °C for the composites after heat treatment for 6 h with 91 wt% inorganic fillers. Fig. 10 shows the synthetic process of TE slurry [61].

Du et al. [43] prepared composites of tungsten carbide (WC)/PLA with different WC volume ratios using an SP process (Fig. 11). As the WC volume ratios increased from ~33% to 60%, the Seebeck coefficients and thermal conductivities ranged from − 11 μV/K to − 12.3 μV/K, and from ~0.2 $Wm^{-1}K^{-1}$ to 0.28 $Wm^{-1}K^{-1}$, respectively, while the electrical conductivity increased from 10.6 S/cm to 42.2 S/cm at 300 K. As a result, a *ZT* value of ~6.7×10^{-4} at 300 K was achieved for composites with ~60 vol% WC [43]. It was the first time flexible n-type polymer-based composites were prepared via an SP process, although the *ZT* value of the WC/PLA composite was relatively low. Recently, we fabricated flexible ternary carbon black/Bi_2Te_3 based alloy/polylactic acid (CB/BTBA/PLA) composites via an SP process [62]. As the content of BTBAs increased from 38.5 wt% to 71.4 wt%, the Seebeck coefficient of the CB/BTBA/PLA composites increased significantly from 60.2 μV/K to 119.9 μV/K, and the electrical conductivity and thermal conductivity increased slightly from 5.8 S/cm to 13.3 S/cm, and from 0.15 $Wm^{-1}K^{-1}$ to 0.25 $Wm^{-1}K^{-1}$, respectively. The *ZT* value increased from 0.004 to 0.023 at 300 K (Fig. 12).

Compared to SLA, FDM, and SLM/SLS additive manufacturing, the SP process has many advantages. SP can print almost any solution that contains inorganic fillers and polymer matrixes in intricate geometries of designed TE composites. SP does not require high temperatures to melt polymers, and it therefore avoids oxidizing inorganic TE materials because the samples are printed at room temperature. Consequently, the SP process has great potential for use with TE materials and devices. The primary obstacle for the SP process is developing inks with high TE properties and suitable viscosity.

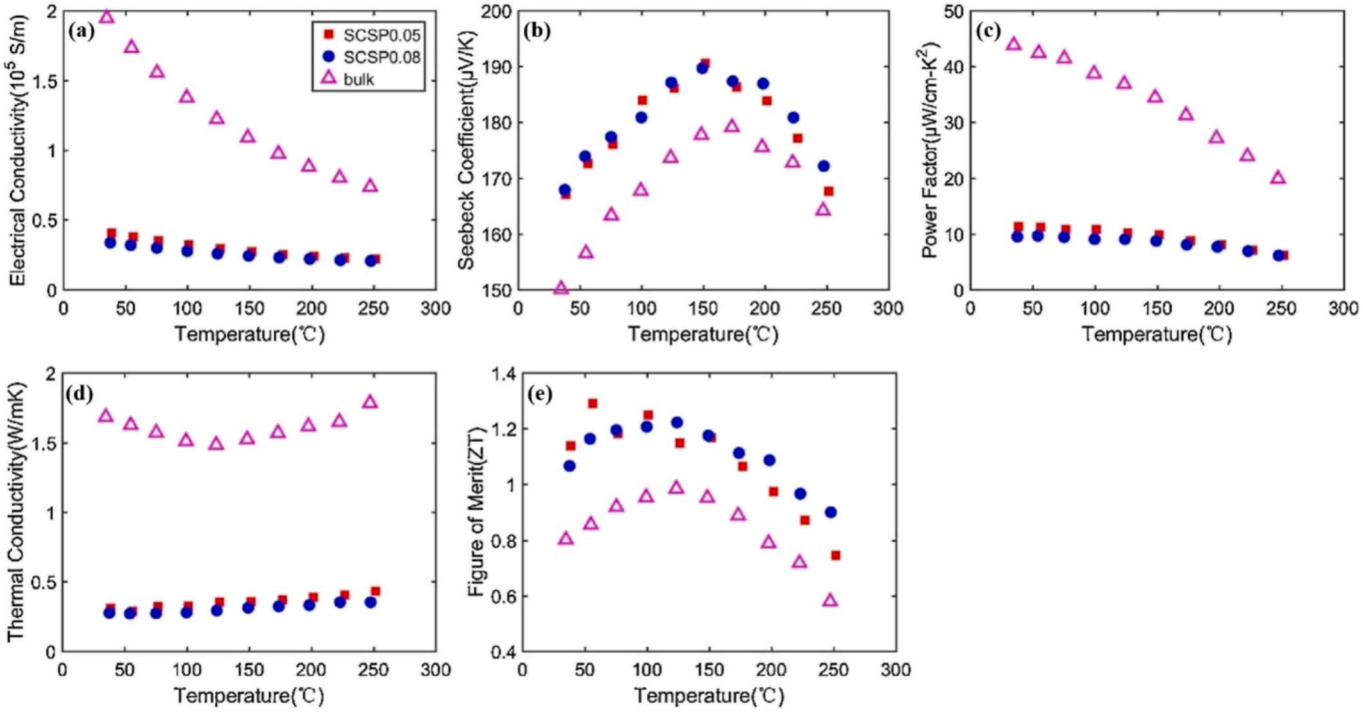

Fig. 9. Temperature dependence of electrical conductivity (a), Seebeck coefficient (b), power factor (c), thermal conductivity (d), and figure of merit (e) of SLS porous sample (red solid square and blue solid circle respectively denotes scan spacing is 0.05 mm and 0.08 mm) as compared with that of commercial bulk (BST bulk). From Ref. [38]. © Elsevier, used with permission. (For interpretation of the references to colour in this figure legend, the reader is referred to the Web version of this article.)

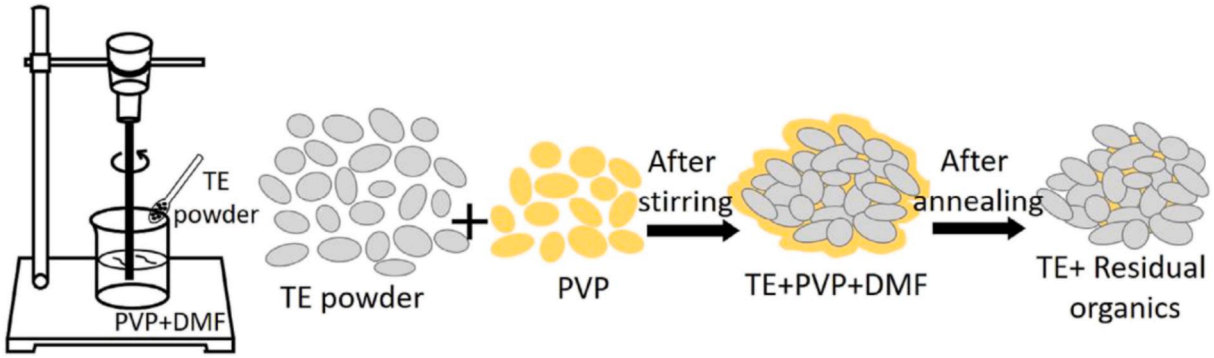

Fig. 10. Schematic illustration of the synthetic process of the TE slurry. From Ref. [61]. © Elsevier, used with permission.

4. Challenges, summary, and conclusions

This review aims to provide a summary of the research progress and key findings on TE materials and devices prepared by additive manufacturing. For reference, Table 2 presents a summary of the TE properties of materials prepared via different additive manufacturing techniques covered in this review.

Due to its unique virtues, additive manufacturing could be a potential developing direction of TE materials and devices. The material requirements for different methods of additive manufacturing are varied, and each type of additive manufacturing has advantages and disadvantages. The SLA process is more suitable for photoresins with or without inorganic fillers. Photoresin types are limited, and the content of inorganic TE materials in the photoresins must be strictly controlled. FDM is more suitable for thermoplastic polymers and their corresponding composites with inorganic TE materials as fillers. Bi-Te- and Pb-Te-based alloys are easily oxidized because the temperature for printing TE materials using FDM is always higher than 200 °C. Atmospheric protection may be an effective method to reduce, even eliminate oxidation of inorganic TE materials. Heat treatment and sintering processes need to be optimized. The SLM process is more suitable for metal powders, while the SLS process can be used with polymers, metals, and alloy powders. Insulating polymers are not necessarily needed as binders during the SLM/SLS process; however, these methods generally require heating to fully or nearly melt the powders, which may introduce impure phases or oxidation. The SP process can print intricate geometries of TE composites using almost any solution that contains polymer matrixes and inorganic fillers, and does not require high temperatures to melt polymers. Furthermore, the SP process avoids oxidation of inorganic TE materials by printing samples at room temperature. The primary issue for the SP process is improving TE properties and viscosity of printing ink.

Additive manufacturing can be used for fabrication of TE materials and devices with designed geometric structures. However, to date, the reported TE additive manufacturing is mainly in fabrication of TE materials. Research and development of TE powered generators and coolers

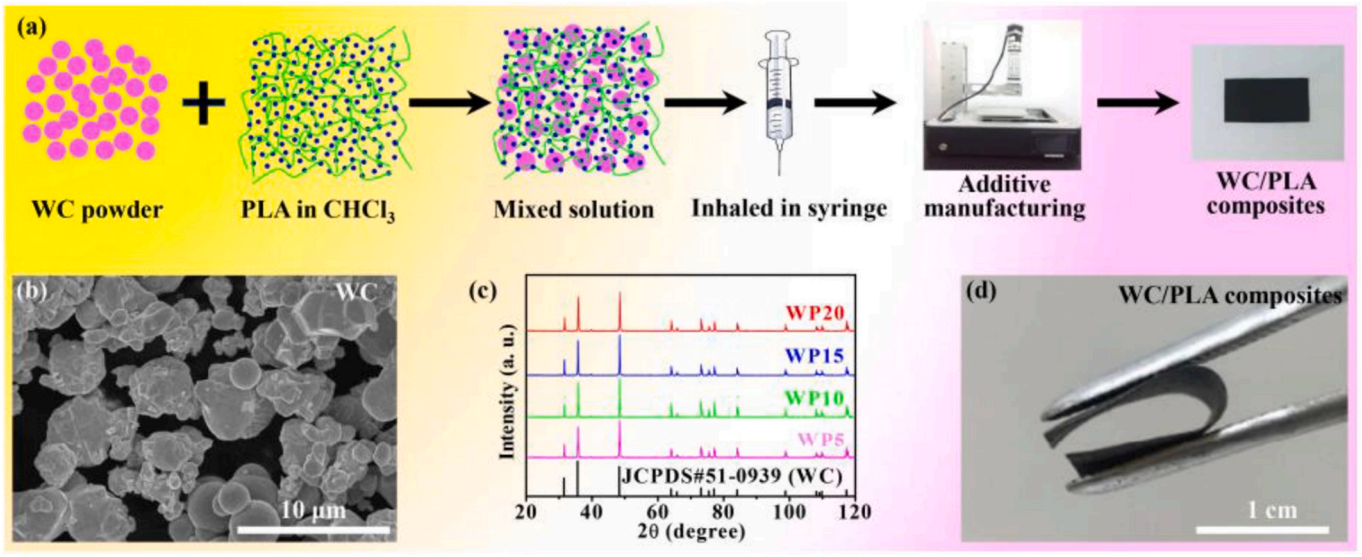

Fig. 11. Schematic of the fabrication process of the WC/PLA thermoelectric composites (a), SEM image of tungsten carbide (WC) (b), XRD patterns of tungsten carbide/polylactic acid (WC/PLA) composites with different WC loadings (c), and the flexible display digital photo of the WP5 (d). The WC/PLA composites with the WC/PLA mass ratios of 5:0.8, 10:0.8, 15:0.8, and 20:0.8 were denoted as WP5, WP10, WP15, and WP20, respectively. From Ref. [43]. Used under CC-BY license.

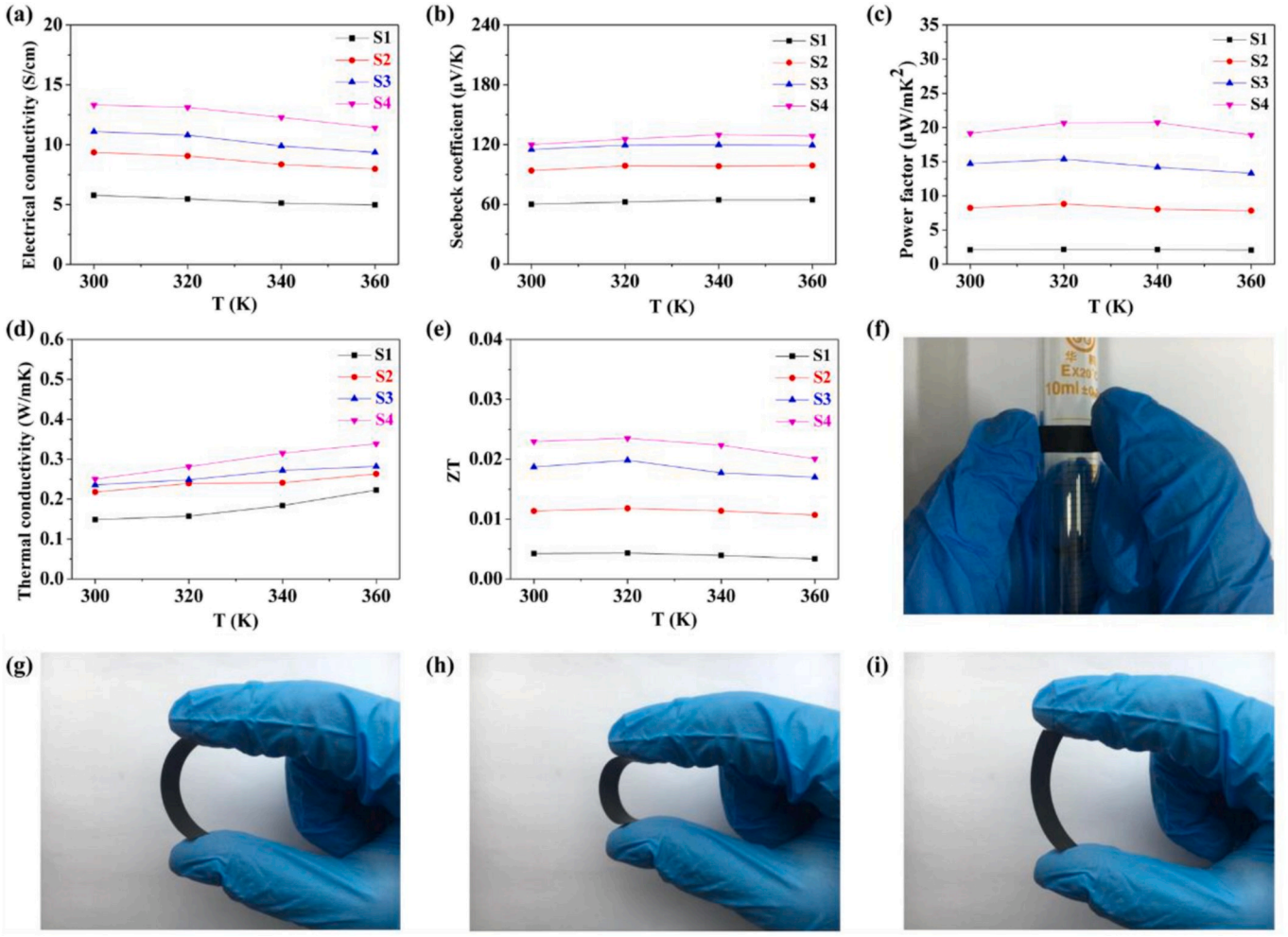

Fig. 12. Electrical conductivity (a), Seebeck coefficient (b), power factor (c), thermal conductivity (d), *ZT* (e) of the CB/BTBA/PLA thermoelectric composites. Flexible display digital photos of the S3 (f) - (i). The mass ratios of PLA:CB:BTBA of 0.5:0.3:0.5, 0.5:0.3:1, 0.5:0.3:1.5, and 0.5:0.3:2 in the CB/BTBA/PLA composites were denoted as S1, S2, S3, and S4, respectively. From Ref. [62]. Used under CC-BY license.

Table 2
The TE properties of materials prepared via different additive manufacturing techniques covered in this review.

Year and Author	Material	Technique	Post process	Electric conductivity (S/cm)	Seebeck coefficient (μV/K)	Thermal conductivity ($Wm^{-1}K^{-1}$)	ZT_{max}
2015, He et al. [39]	$Bi_{0.5}Sb_{1.5}Te_3$/resin composites with 60 wt% $Bi_{0.5}Sb_{1.5}Te_3$	SLA	Annealed at 350 °C in argon gas for 6 h	~ 47 - 33 (43 - 300 °C)	~ 148 - 181 (43 - 300 °C)	~ 0.27–0.81 (43 - 300 °C)	0.12 (43 °C)
2018, Aw et al. [41]	CABS/ZnO composites with 14 wt % ZnO	FDM		3.74×10^{-6} (RT)	2.2 (RT)	0.317 (RT)	5.7×10^{-5} (RT)
2019, Oztan et al. [40]	Bi_2Te_3/ABS composites with 80 wt% Bi_2Te_3	FDM	Heat treatment and sintering at 500 °C for 2 h in ultra-high purity argon environment	54.66–29.44 (RT - 250 °C)	~ 251 - 162 (RT - 250 °C)	~ 0.17–0.44 (RT - 250 °C)	0.54 (RT)
2017, Mao et al. [53]	$Bi_2Te_{2.7}Se_{0.3}$	SLM	Annealing at 673 K for 36 h	~ 830 - 430 (300 - 550 K)	~ - 156 - -177 (300 - 550 K)	~ 0.66–0.12 (300 - 550 K)	0.84 (400 K)
2019. Qiu et al. [60]	$Bi_{0.4}Sb_{1.6}Te_3$	SLM	Vacuum annealing treatment at 673 K for 24 h	~ 1180 - 580 (RT - 525 K)	~ 195 - 90 (316 K–525 K)	~ 1.1–1.6 (316 K–525 K)	1.1 (316 K)
2019, Shi et al. [38]	$Bi_{0.5}Sb_{1.5}Te_3$	SLS		~ 400 - 210 (25 - 250 °C)	~ 168 - 190 (25 - 250 °C)	~ 0.27–0.42 (25 - 250 °C)	1.29 (54 °C)
2018, Kim et al. [42]	$Bi_{0.4}Sb_{1.6}Te_3$	SP	Dried at 105 °C for 12 h before annealing at 450 °C for 1 h in N_2 atmosphere	~ 550 - 230 (25 - 225 °C)	~ 166 - 200 (25 - 225 °C)	~ 0.54–0.63 (25 - 225 °C)	0.9 (125 °C)
	$Bi_{2.0}Te_{2.7}Se_{0.3}$	SP	Dried at 105 °C for 12 h before annealing at 450 °C for 1 h in N_2 atmosphere	~ 500 - 280 (25 - 225 °C)	~ 118 - 145 (25 -225 °C)	~ 0.50–0.56 (25 - 225 °C)	0.6 (170 °C)
2020, Su et al. [61]	Bi_2Te_3/PVP composites with 91 wt% Bi_2Te_3	Direct-writing 3D printing	Heat treatment for 6 h.	~ 103- 52 (25 - 300 °C)	~-135 - -110 (25 - 300 °C)	~ 0.53–0.55 (25 - 300 °C)	0.11 (25 °C)
	$Bi_{0.5}Sb_{1.5}Te_3$/PVP composites with 91 wt% $Bi_{0.5}Sb_{1.5}Te_3$	Direct-writing 3D printing	Heat treatment for 6 h.	~ 81 - 49 (25 - 300 °C)	~ 145 - 120 (25 - 300 °C)	~ 0.51–0.53 (25 - 300 °C)	0.104 (25 °C)
2018, Du et al. [43]	WC/PLA composites with ~ 60 vol % WC	SP	Dried at 60 °C for 12 h	51.1–22.9 (150 - 375 K)	−10.8 - -12.2 (150 - 375 K)	0.28–0.32 (300 - 375 K)	6.7×10^{-4} (300 K)
2020, Du et al. [62]	CB/BTBA/PLA composites with 71.4 wt% BTBAs	SP	Dried at room temperature for 12 h	13.3–11.4 (300 - 360 K)	119.9–128.6 (300 - 360 K)	0.25–0.34 (300 - 360 K)	0.024 (320 K)

and flexible TE devices fabricated by additive manufacturing are urgently needed.

The surfaces of the TE materials prepared by additive manufacturing may not be as smooth as those of traditional manufacturing processes such as hot pressing, spark plasma sintering, and zone melting. It is mainly due to that the print resolutions of additive manufacturing are limited, therefore the print resolutions of additive manufacturing need to be enhanced.

Theoretical simulation and calculation could accurate the research progress of TE materials and device fabrication by additive manufacturing, guiding choices of polymer matrixes and inorganic fillers, selecting appropriate morphologies for inorganic fillers, optimizing the content of each component, and designing and optimizing geometric structures of TE devices. Therefore more theoretical research work on simulation and calculation are expected.

Declaration of competing interest

The authors declare that they have no known competing financial interests or personal relationships that could have appeared to influence the work reported in this paper.

Acknowledgments

This work has been supported by the Shanghai Innovation Action Plan Project (17090503600), the National Natural Science Foundation of China (11811530636, 61504081, 61611530550), and the Program for Professor of Special Appointment (Young Eastern Scholar Program) at Shanghai Institutions of Higher Learning (QD2015039).

References

[1] T.J. Seebeck, Magnetische polarisation der metalle und erze durchtemperatur-differenz, Abh. Akad. Wiss. Berlin 1820–21 (1822) 289–346.
[2] D.M. Rowe, CRC Handbook of Thermoelectrics, CRC Press, 1995.
[3] L.E. Bell, Cooling, heating, generating power, and recovering waste heat with thermoelectric systems, Science 321 (2008) 1457–1461.
[4] Y. Du, J.Y. Xu, B. Paul, P. Eklund, Flexible thermoelectric materials and devices, Appl. Mater. Today 12 (2018) 366–388.
[5] G.J. Snyder, E.S. Toberer, Complex thermoelectric materials, Nat. Mater. 7 (2008) 105–114.
[6] X. Zhang, L.D. Zhao, Thermoelectric materials: energy conversion between heat and electricity, J. Materiomics 1 (2015) 92–105.
[7] R. He, G. Schierning, K. Nielsch, Thermoelectric devices: a review of devices, architectures, and contact optimization, Adv. Mater. Technol. 3 (2018) 1700256.
[8] L.D. Zhao, S.H. Lo, Y.S. Zhang, H. Sun, G.J. Tan, C. Uher, C. Wolverton, V. P. Dravid, M.G. Kanatzidis, Ultralow thermal conductivity and high thermoelectric figure of merit in SnSe crystals, Nature 508 (2014) 373–377.
[9] J.P. Heremans, V. Jovovic, E.S. Toberer, A. Saramat, K. Kurosaki, A. Charoenphakdee, S. Yamanaka, G.J. Snyder, Enhancement of thermoelectric efficiency in PbTe by distortion of the electronic density of states, Science 321 (2008) 554–557.
[10] B. Poudel, Q. Hao, Y. Ma, Y.C. Lan, A. Minnich, B. Yu, X. Yan, D.Z. Wang, A. Muto, D. Vashaee, X.Y. Chen, J.M. Liu, M.S. Dresselhaus, G. Chen, Z.F. Ren, High-thermoelectric performance of nanostructured bismuth antimony telluride bulk alloys, Science 320 (2008) 634–638.
[11] B. Paul, J. Lu, P. Eklund, Nanostructural tailoring to induce flexibility in thermoelectric $Ca_3Co_4O_9$ thin films, ACS Appl. Mater. Interfaces 9 (2017) 25308–25316.
[12] P. Eklund, S. Kerdsongpanya, B. Alling, Transition-metal-nitride-based thin films as novel energy harvesting materials, J. Mater. Chem. C 4 (2016) 3905–3914.
[13] G.H. Kim, L. Shao, K. Zhang, K.P. Pipe, Engineered doping of organic semiconductors for enhanced thermoelectric efficiency, Nat. Mater. 12 (2013) 719–723.

[14] O. Bubnova, Z.U. Khan, A. Malti, S. Braun, M. Fahlman, M. Berggren, X. Crispin, Optimization of the thermoelectric figure of merit in the conducting polymer poly (3,4-ethylenedioxythiophene), Nat. Mater. 10 (2011) 429–433.

[15] O. Bubnova, Z.U. Khan, H. Wang, S. Braun, D.R. Evans, M. Fabretto, P. Hojati-Talemi, D. Dagnelund, J.-B. Arlin, Y.H. Geerts, S. Desbief, D.W. Breiby, J. W. Andreasen, R. Lazzaroni, W.M. Chen, I. Zozoulenko, M. Fahlman, P.J. Murphy, M. Berggren, X. Crispin, Semi-metallic polymers, Nat. Mater. 13 (2014) 190–194.

[16] Y. Du, K.F. Cai, S. Chen, P. Cizek, T. Lin, Facile preparation and thermoelectric properties of Bi_2Te_3 based alloy nanosheet/PEDOT:PSS composite films, ACS Appl. Mater. Interfaces 6 (2014) 5735–5743.

[17] K.C. See, J.P. Feser, C.E. Chen, A. Majumdar, J.J. Urban, R.A. Segalman, Water-processable polymer-nanocrystal hybrids for thermoelectrics, Nano Lett. 10 (2010) 4664–4667.

[18] Y. Du, X. Liu, J.Y. Xu, S.Z. Shen, Flexible Bi–Te-based alloy nanosheet/PEDOT: PSS thermoelectric power generators, Mater. Chem. Front. 3 (2019) 1328–1334.

[19] H. Ju, J. Kim, Chemically exfoliated SnSe nanosheets and their SnSe/poly (3, 4-ethylenedioxythiophene):poly(styrenesulfonate) composite films for polymer based thermoelectric applications, ACS Nano 10 (2016) 5730–5739.

[20] Y. Du, S.Z. Shen, K.F. Cai, P.S. Casey, Research progress on polymer-inorganic thermoelectric nanocomposite materials, Prog. Polym. Sci. 37 (2012) 820–841.

[21] J. Peng, I. Witting, N. Geisendorfer, M. Wang, M. Chang, A. Jakus, C. Kenel, X. Yan, R. Shah, G.J. Snyder, M. Grayson, 3D extruded composite thermoelectric threads for flexible energy harvesting, Nat. Commun. 10 (2019) 5590.

[22] J.W. Fergus, Oxide materials for high temperature thermoelectric energy conversion, J. Eur. Ceram. Soc. 32 (2012) 525–540.

[23] L.C. Chen, P.Q. Chen, W.J. Li, Q. Zhang, V.V. Struzhkin, A.F. Goncharov, Z.F. Ren, X.J. Chen, Enhancement of thermoelectric performance across the topological phase transition in dense lead selenide, Nat. Mater. 18 (2019) 1321–1326.

[24] Y. Du, K.F. Cai, H. Li, B.J. An, The influence of sintering temperature on the microstructure and thermoelectric properties of n-type $Bi_2Te_{3-x}Se_x$ nanomaterials, J. Electron. Mater. 40 (2011) 518–522.

[25] H. Wang, Y.Z. Pei, A.D. LaLonde, G.J. Snyder, Weak electron–phonon coupling contributing to high thermoelectric performance in n-type PbSe, Proc. Natl. Acad. Sci. Unit. States Am. 109 (2012) 9705–9709.

[26] S.L. Sun, J. Peng, R.X. Jin, S.Y. Song, P.W. Zhu, Y. Xing, Template-free solvothermal synthesis and enhanced thermoelectric performance of Sb_2Te_3 nanosheets, J. Alloys Compd. 558 (2013) 6–10.

[27] L.D. Zhao, H. Wu, S. Hao, C.I. Wu, X. Zhou, K. Biswas, J. He, T.P. Hogan, C. Uher, C. Wolverton, All-scale hierarchical thermoelectrics: MgTe in PbTe facilitates valence band convergence and suppresses bipolar thermal transport for high performance, Energy Environ. Sci. 6 (2013) 3346–3355.

[28] H.J. Wu, L.D. Zhao, F.S. Zheng, D. Wu, Y.L. Pei, X. Tong, M.G. Kanatzidis, J.Q. He, Broad temperature plateau for thermoelectric figure of merit $ZT > 2$ in phase-separated $PbTe_{0.7}S_{0.3}$, Nat. Commun. 5 (2014) 4515.

[29] J. Jiang, L.D. Chen, Q. Yao, S.Q. Bai, Q. Wang, Effect of TeI_4 content on the thermoelectric properties of n-type Bi-Te-Se crystals prepared by zone melting, Mater. Chem. Phys. 92 (2005) 39–42.

[30] G. Kavei, M.A. Karami, Fabrication and characterization of the p-type $(Bi_2Te_3)_x(Sb_2Te_3)_{1-x}$ thermoelectric crystals prepared via zone melting, Bull. Mater. Sci. 29 (2006) 659–663.

[31] L. Yuan, S.L. Ding, C. Wen, Additive manufacturing technology for porous metal implant applications and triple minimal surface structures: a review, Bioact. Mater. 4 (2019) 56–70.

[32] D.D. Camacho, P. Clayton, W.J. O'Brien, C. Seepersad, M. Juenger, R. Ferron, S. Salamone, Applications of additive manufacturing in the construction industry–A forward-looking review, Autom. ConStruct. 89 (2018) 110–119.

[33] S. Singh, S. Ramakrishna, R. Singh, Material issues in additive manufacturing: a review, J. Manuf. Process. 25 (2017) 185–200.

[34] A.N. Dickson, J.N. Barry, K.A. McDonnell, D.P. Dowling, Fabrication of continuous carbon, glass and Kevlar fibre reinforced polymer composites using additive manufacturing, Addit. Manuf. 16 (2017) 146–152.

[35] K. Gnanasekaran, T. Heijmans, S. Van Bennekom, H. Woldhuis, S. Wijnia, G. de With, H. Friedrich, 3D printing of CNT-and graphene-based conductive polymer nanocomposites by fused deposition modeling, Appl. Mater. Today 9 (2017) 21–28.

[36] S.J. Leigh, R.J. Bradley, C.P. Purssell, D.R. Billson, D.A. Hutchins, A simple, low-cost conductive composite material for 3D printing of electronic sensors, PloS One 7 (2012) 1–6.

[37] Y.W. Zhai, D.A. Lados, J.L. LaGoy, Additive manufacturing: making imagination the major limitation, JOM (J. Occup. Med.) 66 (2014) 808–816.

[38] J.X. Shi, H.L. Chen, S.H. Jia, W.J. Wang, 3D printing fabrication of porous bismuth antimony telluride and study of the thermoelectric properties, J. Manuf. Process. 37 (2019) 370–375.

[39] M.H. He, Y. Zhao, B. Wang, Q. Xi, J. Zhou, Z.Q. Liang, 3D printing fabrication of amorphous thermoelectric materials with ultralow thermal conductivity, Small 11 (2015) 5889–5894.

[40] C. Oztan, S. Ballikaya, U. Ozgun, R. Karkkainen, E. Celik, Additive manufacturing of thermoelectric materials via fused filament fabrication, Appl. Mater. Today 15 (2019) 77–82.

[41] Y.Y. Aw, C.K. Yeoh, M.A. Idris, P.L. Teh, K.A. Hamzah, S.A. Sazali, Effect of printing parameters on tensile, dynamic mechanical, and thermoelectric properties of FDM 3D printed CABS/ZnO composites, Materials 11 (2018) 466.

[42] F. Kim, B. Kwon, Y. Eom, J.E. Lee, S. Park, S. Jo, S.H. Park, B.-S. Kim, H.J. Im, M. H. Lee, T.S. Min, K.T. Kim, H.G. Chae, W.P. King, J.S. Son, 3D printing of shape-conformable thermoelectric materials using all-inorganic Bi_2Te_3-based inks, Nat. Energy 3 (2018) 301–309.

[43] Y. Du, J.G. Chen, X. Liu, C. Lu, J.Y. Xu, B. Paul, P. Eklund, Flexible n-type tungsten carbide/polylactic acid thermoelectric composites fabricated by additive manufacturing, Coatings 8 (2018) 25.

[44] S.C. Ligon, R. Liska, J.r. Stampfl, M. Gurr, R. Mülhaupt, Polymers for 3D printing and customized additive manufacturing, Chem. Rev. 117 (2017) 10212–10290.

[45] J.R.C. Dizon, A.H. Espera Jr., Q.Y. Chen, R.C. Advincula, Mechanical characterization of 3D-printed polymers, Addit. Manuf. 20 (2018) 44–67.

[46] T.D. Ngo, A. Kashani, G. Imbalzano, K.T.Q. Nguyen, D. Hui, Additive manufacturing (3D printing): a review of materials, methods, applications and challenges, Compos. B Eng. 143 (2018) 172–196.

[47] H.N. Chia, B.M. Wu, Recent advances in 3D printing of biomaterials, J. Biol. Eng. 9 (2015) 4.

[48] B.C. Gross, J.L. Erkal, S.Y. Lockwood, C.P. Chen, D.M. Spence, Evaluation of 3D printing and its potential impact on biotechnology and the chemical sciences, Anal. Chem. 86 (2014) 3240–3253.

[49] F. Rengier, A. Mehndiratta, H. Von Tengg-Kobligk, C.M. Zechmann, R. Unterhinninghofen, H.-U. Kauczor, F.L. Giesel, 3D printing based on imaging data: review of medical applications, Int. J. CARS 5 (2010) 335–341.

[50] S. Bose, S. Vahabzadeh, A. Bandyopadhyay, Bone tissue engineering using 3D printing, Mater. Today 16 (2013) 496–504.

[51] X. Wang, M. Jiang, Z.W. Zhou, J.H. Gou, D. Hui, 3D printing of polymer matrix composites: a review and prospective, Compos. B Eng. 110 (2017) 442–458.

[52] T.L. Chen, C. Luo, Y.G. Yan, J.H. Yang, Q.J. Zhang, C. Uher, X.F. Tang, Rapid fabrication and thermoelectric performance of SnTe via non-equilibrium laser 3D printing, Rare Met. 37 (2018) 300–307.

[53] Y. Mao, Y.G. Yan, K.P. Wu, H.Y. Xie, Z.K. Xiu, J.H. Yang, Q.J. Zhang, C. Uher, X. F. Tang, Non-equilibrium synthesis and characterization of n-type $Bi_2Te_{2.7}Se_{0.3}$ thermoelectric material prepared by rapid laser melting and solidification, RSC Adv. 7 (2017) 21439–21445.

[54] K.V. Wong, A. Hernandez, A review of additive manufacturing, ISRN Mech. Eng. 2012 (2012) 208760.

[55] V. Tambrallimath, R. Keshavamurthy, D. Saravanabavan, P.G. Koppad, G. S. Pradeep Kumar, Thermal behavior of PC-ABS based graphene filled polymer nanocomposite synthesized by FDM process, Compos. Commun. 15 (2019) 129–134.

[56] S. Dul, L. Fambri, A. Pegoretti, Fused deposition modelling with ABS–graphene nanocomposites, Compos. Part A-Appl. S. 85 (2016) 181–191.

[57] J.C. Camargo, Á.R. Machado, E.C. Almeida, E.F.M.S. Silva, Mechanical properties of PLA-graphene filament for FDM 3D printing, Int. J. Adv. Manuf. Technol. 103 (2019) 2423–2443.

[58] J.Z. Wang, H.Z. Li, R.X. Liu, L.L. Li, Y.H. Lin, C.W. Nan, Thermoelectric and mechanical properties of PLA/$Bi_{0.5}Sb_{1.5}Te_3$ composite wires used for 3D printing, Compos. Sci. Technol. 157 (2018) 1–9.

[59] K. Kempen, E. Yasa, L. Thijs, J.-P. Kruth, J. Van Humbeeck, Microstructure and mechanical properties of selective laser melted 18Ni-300 steel, Phys. Procedia 12 (2011) 255–263.

[60] J.H. Qiu, Y.G. Yan, T.T. Luo, K.C. Tang, L. Yao, J. Zhang, M. Zhang, X.L. Su, G. J. Tan, H.G. Xie, M.G. Kanatzidis, C. Uher, X.F. Tang, 3D Printing of highly textured bulk thermoelectric materials: mechanically robust BiSbTe alloys with superior performance, Energy Environ. Sci. 12 (2019) 3106–3117.

[61] N. Su, P.F. Zhu, Y.H. Pan, F. Li, B. Li, 3D-printing of shape-controllable thermoelectric devices with enhanced output performance, Energy 195 (2020) 116892.

[62] Y. Du, J.G. Chen, Q.F. Meng, J.Y. Xu, B. Paul, P. Eklund, Flexible ternary carbon black/Bi_2Te_3 based alloy/polylactic acid thermoelectric composites fabricated by additive manufacturing, J. Materiomics 6 (2020) 293–299.